Materials Horizons



COMMUNICATION

View Article Online



Cite this: Mater. Horiz., 2023, 10.2047

Received 18th October 2022, Accepted 3rd April 2023

DOI: 10.1039/d2mh01293f

rsc li/materials-horizons

Controlling selectivity for dechlorination of poly(vinyl chloride) with (xantphos)RhCl†

Nancy G. Bush, 📵 ‡ a Mikiyas K. Assefa, 📵 ‡ a Selin Bac, 📵 b Shaama Mallikarjun Sharada 🕩 *ab and Megan E. Fieser 🕩 *ac

Reaction of poly(vinyl chloride) (PVC) with 5 equiv. of triethyl silane in THF, in the presence of in situ generated (xantphos)RhCl catalyst, results in partial reduction of PVC via hydrodechlorination to yield poly(vinyl chloride-co-ethylene). Increasing catalyst loading or using N,N-dimethylacetamide (DMA) as a solvent both diminished selectivity for hydrodechlorination, promoting competitive dehydrochlorination reactions. Reaction of PVC with 2 equiv. of sodium formate in THF in the presence of (xantphos)RhCl affords excellent selectivity for hydrodechlorination along with complete PVC dechlorination, yielding polyethylene-like polymers. Higher catalyst loadings were necessary to activate PVC towards reduction in this case. In contrast, reaction of PVC with 1 equiv. of NaH in DMA, in the presence of (xantphos)RhCl, exhibited good selectivity for dehydrochlorination, as well as much higher reaction rates. These results combined shed light on the interplay between critical reaction parameters that control PVC's mode of reactivity.

Introduction

Poly(vinyl chloride) (PVC) is the third most produced polymer, behind polyethylene and polypropylene, and is used extensively in construction and medical fields. With such a large production scale, there is still poor recovery of materials from PVC mechanical recycling.2 The majority of PVC waste is incinerated, disposed to landfill, or leaked into the environment,

‡ Authors contributed equally.

New concepts

Poly(vinyl chloride) is critical to many industries, yet has no widespread methods for commercial mechanical or chemical recycling due to complications from the chlorine in its backbone and a wide variety of additives across products. Previous methods have focused on dechlorination as a pretreatment to pyrolysis or downcycling methods with little interest in the dechlorinated organic product. When organic products were characterized, dehydrochlorination led to unstable polyacetylene-like polymers with little use. We identify the first example of using a molecular inorganic catalyst to control the dechlorination reactivity of PVC to perform hydrodechlorination to form polyethylenelike materials. Not only can all chlorine be eliminated, but side reactions caused by base-mediated dehydrochlorination can be suppressed leading to high selectivity for polyethylene using optimized conditions. Guided by theoretical calculations, the effects of various solvents and hydride donors were explored to gain better understanding of how reaction conditions impact dechlorination pathways. This will open new avenues for the efficient and controlled upcycling of PVC to a variety of products. Finally, this method was successful in partially dechlorinating commercial PVC products despite dyes, paints and plasticizers being present. These results show a promising robustness in the catalyst across the vast array of PVC materials.

generating environmentally harmful dioxins and HCl gas.3,4 Moreover, if PVC is added to mixed plastics recycling, it is difficult to separate from polyolefin mixtures. With the generation of HCl at high temperatures, even small impurities of PVC cause corrosion of pyrolysis reactors or deactivation of pyrolysis catalysts.5,6

While mechanical recycling is feasible for certain PVC materials, the use of various additives in PVC products requires extensive pre-sorting to maintain polymer properties when recycled. Instead, chemical dehydrochlorination (DHC) without formation of HCl has proved a useful pre-treatment before pyrolysis. While Cl is removed from the polymer chain, the complexity of the dechlorination methods employed often requires extreme conditions and the organic polymer fragment is not prioritized. In addition, complete dechlorination of PVC has been difficult to achieve via DHC.8 We have recently reported a method to convert PVC to poly(ethylene-co-styrenic) copolymers,

^a Department of Chemistry, University of Southern California, Los Angeles, California 90089, USA

^b Department of Chemical Engineering and Materials Science, Mork Family, University of Southern California, Los Angeles, California 90089, USA. E-mail: ssharada@usc.edu

^c Wrigley Institute for Environmental Studies, University of Southern California, Los Angeles, California 90089, USA. E-mail: fieser@usc.edu

[†] Electronic supplementary information (ESI) available: Catalyst synthesis, catalytic conditions, characterization data (AT-IR, NMR, DSC, TGA, SEM-EDX) and crystal structure data. CCDC 2213615. For ESI and crystallographic data in CIF or other electronic format see DOI: https://doi.org/10.1039/d2mh01293f

Communication **Materials Horizons**

Prior and current catalysts and reagents used to hydrodechlorinate PVC.

with full dechlorination of PVC within minutes. While these copolymers can serve in high value applications, the presence of aromatic substituents may not be desired and full conversion to a single homopolymer would be useful.

Selective hydrodechlorination (HDC), or reduction, of PVC is an attractive route to remove Cl from the polymer, leaving valuable polyethylene (PE)-like materials behind (Fig. 1). This strategy could be useful for PE waste to convert PVC impurities to PE prior to pyrolysis or mechanical recycling. However, studies to establish control over product selectivity for this process are limited. Indeed, while tributyl tin hydride, lithium aluminium hydride and super hydride have been used to stoichiometrically reduce PVC to PE-like materials (Fig. 1a), these examples suffered from low lifetimes of the radical initiators employed at elevated temperatures, as well as poor selectivity where competitive dehydrochlorination reactions were evident to varying degrees for the different hydrides. 9-15 Recently, Cantat and coworkers used Brookhart's catalyst to hydrodechlorinate PVC with triethylsilane, in which triethylsilyl chloride was generated at mild temperatures (Fig. 1b).16 However, only one reaction in a J-Young tube was performed, and the reduced organic product was never characterized by any means. Further, the chlorobenzene solvent used was likely a competitive substrate for hydrodechlorination, and selectivity for HDC versus DHC was not investigated. Nevertheless, this study demonstrated the role of catalysts for efficient dechlorination at low temperatures.

Rhodium complexes have recently been identified as promising catalysts for the activation of C(sp³)-Cl bonds.¹⁷ Most notable are Rh^I catalysts supported on xantphos (POP)-based ligands, which proved effective for hydrodechlorination of Clcontaining small molecules. We aimed to investigate if these complexes could be extended for use on PVC materials. Our recent computational studies to this end found POP^RRhCl catalysts could promote selectivity for HDC of PVC, in the presence of hydride donors such as sodium hydride or sodium formate.18

Herein, we demonstrate experimental evidence that (xantphos) RhCl catalysts (where xantphos = POPPh) can promote controlled HDC of PVC with different hydride donors at mild temperatures (Fig. 1b). Surprising impacts of solvent choice, catalyst loading, and hydride donor on the degree and selectivity of dechlorination are reported.

Results and discussion

For this study, we aimed to employ a fast characterization method that could quickly reveal the degree of dechlorination and the selectivity for HDC over DHC for a particular reaction condition. As such, ATR-IR spectroscopy was chosen as an initial screening tool for qualitative assessment of dechlorination reactions, as the IR spectra for polyethylene (PE), polyacetylene (PA) and PVC all exhibit distinct vibrational features. Selected reactions were subsequently analysed by ¹H NMR spectroscopy, elemental analysis, differential scanning calorimetry (DSC), thermogravimetric analysis (TGA), and energy dispersive X-ray spectroscopy (EDX). Mechanistic findings from the previous computational study were employed to calculate solvent-sensitivity. In addition, the energetics of direct, concerted dehydrochlorination by various salts were calculated.

Drawing inspiration from the works of Cantat and our prior computational studies, PVC hydrodechlorination was attempted using triethylsilane, sodium formate, and sodium hydride as hydrogen donors with a POPPhRhCl catalyst generated in situ in tetrahydrofuran (THF) at 110 °C (Fig. 2). THF was selected as a suitable solvent as it can readily dissolve PVC even at room temperature.19 If successful, Cl-containing by-products from these reactions would be innocuous NaCl and valuable silyl source, Et₃SiCl.²⁰ For full details of condition optimization, see the ESI.†

HDC of PVC at 1 mol% catalyst loading in the presence of 5 equiv. of Et₃SiH for 2 d at 110 °C resulted in an IR spectrum resembling an overlay of those for PVC and PE (Fig. 3). Notably, no obvious C=C stretches in 1600-1700 cm⁻¹ are visible, consistent with good selectivity for HDC. Formation of ethylene sequences was corroborated by the appearance of peaks at 1459 and 721 cm⁻¹ ascribable to CH₂ bending and rocking vibrations, respectively, for $(CH_2)_n$ sequences where $n \ge 5.15,21-23$ The ¹H NMR spectrum of the resulting product revealed a series of resonances at 3.8-4.7 ppm assignable to CHCl proton environments that correspond to meso and racemic combinations of vinyl chloride in VV diads (V = vinyl chloride) (Fig. S31, ESI†). 23-28

Fig. 2 Experimental methods for PVC dechlorination with different H sources (Et₃SiH, NaHCO₂, and NaH) and solvents (THF and N,Ndimethylacetamide, DMA).

Materials Horizons Communication

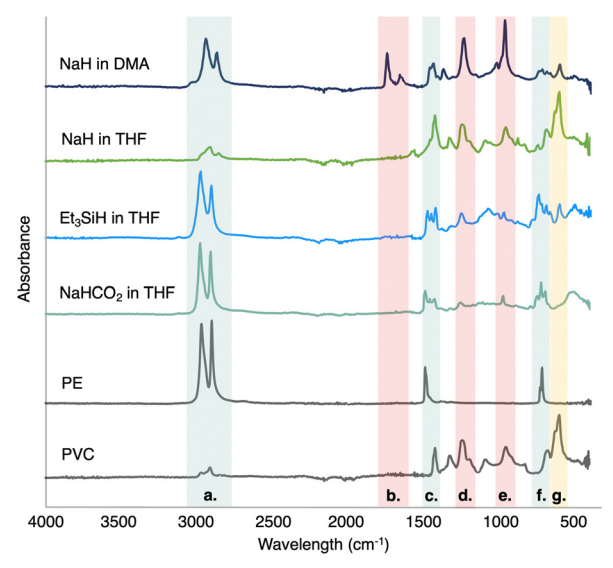


Fig. 3 ATR-IR data of dechlorinated PVC for various hydride donors compared to lab grade PVC and PE. Shaded regions a, c, and f highlight the characteristic PE peaks for the symmetric and asymmetric C-H stretching, CH₂ bending and CH₂ rocking vibrations, respectively.²¹ Shaded regions b, d, and e highlight the C=O stretching, C-O stretching, and C=C bending modes as products of undesired side reactions, respectively. Shaded region g highlights the C-Cl stretching mode. Reaction conditions for NaH (1 equiv., 1 mol% [Rh]), NaHCO₂ (2 equiv., 5 mol% [Rh]) or Et₃SiH (5 equiv., 1 mol% [Rh]) (Table S2, ESI,† entries 3a-3b, 2c, and 1a, respectively) at 110 °C for 2d.

Ethylene sequences in VE + EV diads (E = ethylene) are also evident at 1.86 ppm, as are EE diads at 1.26 ppm.²⁹ We also observe minor resonances assignable to olefinic and aromatic environments at 5.40 ppm and 7.3-7.9 ppm.²⁸ Relative integration of these resonances approximate a 63% conversion of PVC to PE has been achieved. Importantly, elemental analysis data (Fig. 4A) of the product was consistent with the formulation obtained from relative integration of the vinyl chloride and ethylene resonances in the ¹H NMR spectrum. A duplicate reaction reveals similar results. Interestingly, increasing the catalyst loading to 5 mol% with 5 equiv. of triethyl silane in THF for 2 d resulted in a much faster consumption of PVC, but with concomitant prevalence of competitive DHC (Fig. S9, ESI†). This may be due to a diminished pre-catalyst activation or the larger catalyst/hydrogen source molar ratio.

For the dechlorination mechanism proposed in the prior computational study, turnover frequencies (TOFs) were calculated at 110 °C for Me₃SiH as the salt and compared to those for NaHCO2 and NaH. 1-Chloropropane was used instead of PVC as the model substrate and the Ph substituents of xantphos were exchanged for methyls (POPMe) to reduce computational time. The comparison with experiment is qualitative on account of the choice of model substrate and catalyst as well as the fact that the TOF method is applicable only to reactions at steady state. The TOF for Me₃SiH in THF $(0.25 h^{-1})$ is 4332 times higher than NaHCO₂ (5.84 \times 10⁻⁵ h⁻¹) and identical to that of NaH. This is because the turnover-determining states and energetic span for cycles with Me₃SiH and NaH are identical

under the assumption (from prior work) that the intrinsic barrier to hydride transfer is less than 120 kJ mol⁻¹.¹⁸

To explain increased DHC of PVC with higher catalyst loadings, methods that promote DHC were pursued. Without the Rh catalyst, methods could not be identified for silanemediated DHC of PVC. Indeed, a control reaction for PVC with 5 equiv. of Et₃SiH for 2 d in THF at 110 °C led to no observable conversion of PVC through HDC or DHC (Fig. S26, ESI†). Alternatively, POP^{Me}RhCl was found to have a high energy pathway towards DHC of PVC without using the silane. To investigate the impacts of catalyst loading on this energy barrier, control reactions carried out using the catalyst alone at 5 mol% loading in THF for 2 d at 110 °C, which revealed incidence of DHC to a small extent (Fig. S24, ESI†). We hypothesize that this is the reason for increased DHC when catalyst loading is increased.

The IR spectra of products from HDC of PVC with 2 equiv. of sodium formate for 2 d in THF at 1 mol% catalyst loading were indicative of slow activation of C-Cl bond in PVC (Fig. S12, ESI†). While only qualitative, this supports the predicted higher TOF for Me₃SiH over NaHCO₂, discussed above. However, increasing the catalyst loading to 5 mol% alongside 2 equiv. of sodium formate for 1 d resulted in significant loss of the C-Cl stretches in the starting PVC (600-650 cm⁻¹), and rise of prominent C-H stretches at 2800-3000 cm⁻¹ ascribable to saturated aliphatic hydrocarbons (Fig. S13, ESI†). The distribution of the latter stretches overlapped significantly with those of PE. Further, CH₂ bending and rocking vibrations at 1462 and 721 cm⁻¹ are reassuring of incorporation of consecutive ethylene sequences along the polymer backbone, on the basis of comparison with the IR spectrum of PE pellets recorded independently.²² Additional minor peaks assignable to unsaturated CH2 out-of-plane bending and deformation vibrational modes were also present, suggestive of competitive DHC reactions. Indeed, poorly defined peaks in the 1000–1300 cm⁻¹ region ascribable to C-O stretches are consistent with formation of conjugated dienes that get oxidized upon quenching of the reaction. Increasing the reaction time to 2 d resulted in complete disappearance of the C-Cl stretches of PVC and growth of those related to PE (Fig. 3). Thus, in contrast to the reactions with Et₃SiH, the use of sodium formate leads to a fast dechlorination (including HDC and DHC) of PVC at higher catalyst loadings while maintaining a good level of control for HDC. A duplicate reaction and reaction scaled up by a factor of 5 showed similar results (see ESI† for comparisons), demonstrating the reproducibility of the reactions.

A control reaction using 2 equiv. sodium formate for 2 d in THF at 110 °C only resulted in exclusive formation of unsaturated and oxidized hydrocarbons (Fig. S28, ESI†). DFT was employed to calculate transition structures for concerted DHC of 1-chloropropane by the salt (NaHCO₂, NaH, SiH₄) alone. The calculated intrinsic barrier to DHC is lowest for NaH $(71.9 \text{ kJ mol}^{-1})$, followed by NaHCO₂ $(100.2 \text{ kJ mol}^{-1})$, and is highest for SiH₄ (249.4 kJ mol⁻¹). Direct DHC by the salt, therefore, is one possible reason why NaHCO2 is less selective towards HDC than triethylsilane per molar equivalent.

Communication

8.0

7.0

6.0

5.0

3.0

40

f1 (ppm)

2.0

1.0

0.0

B. DSC A. **EA Data** H % C % Heat Flow, endo down NaHCO₂a 72.0 10.7 NaH^b 70.5 8.4 Et₃SiH^c 57.5 8.4 $T_m = 94$ °C C. HT-NMR -H₂C-CH₂-20 40 60 80 100 120 140 160 180 Aromatics -HC=CH-Temperature (°C) -C=CH-CH₂-D. SEM-EDX 0.46 0.19 8.0 7.0 6.0 NaHCO₂ 1.00 11.08 residual 2.0 3.0 1.0 Solvent from reaction

Fig. 4 (A) Elemental Analysis (CHNS) data of polymer products from reaction conditions for each hydride donor (based on 1H NMR data, expected EA data for NaHCO₂ is 86.1%C/13.9%H and Et₃SiH is 58.9%C/9.0%H). (B) DSC data for formate polymer product.^a (C) High temperature NMR of formate polymer product in tetrachloroethane-d₂.^a (D) SEM-EDX analysis of formate polymer product.^a Reaction conditions: ^a 5 mol% Rh^{Ph}POPCI, 2 equiv. NaHCO₂ in THF at 110 °C for 2 d (Table S2, ESI,† entry 2c). ^b 1 mol% Rh^{Ph}POPCI, 1 equiv. NaH in DMA at 110 °C for 2 d (Table S2, ESI,† entry 3b). ^c 1 mol% Rh^{Ph}POPCI, 5 equiv. Et₃SiH in THF at 110 °C for 2 d (Table S2, ESI,† entry 1a).

To confirm the formation of a PE-like polymer from HDC of PVC using sodium formate, the product from the above mentioned 2 d reaction was analysed by DSC (Fig. 4B). The DSC curve revealed a T_{m} at 94 °C, a value that is consistent with that for LDPE (100-120 °C). 30,31 Additionally, no T_g is observed within the temperature window used. TGA analysis found $T_{\rm d.5\%}$ of 287 °C, which is somewhat shy of that for LDPE (387 °C). 31,32 Further, the ¹H NMR spectrum of the product in C₂D₂Cl₄ at 110 °C exhibited a major sharp resonance at 1.37 ppm, in agreement with that reported for ethylene sequences in copolymers of vinyl chloride and ethylene (Fig. 4C). 23,27,28 Very minor resonances at 5.4-5.5 and 6.9-7.9 ppm are suggestive of olefinic and aromatic environments, while a minor resonance at 2.04 is attributed to methylene groups adjacent to these environments. Importantly, we do not observe any -CHCl proton environments in this spectrum, implicating near-complete dechlorination. Based on the NMR data, a 92% polyethylene content is approximated. Not all of the polymer product dissolved in the C2D2Cl4 at 110 °C overnight, which could be due to the low solubility of PE or due to unknown crosslinking. This indicated that more bulk analysis would be useful. EA of the polymeric product revealed wt% C and wt% H values that were lower than that for the composition calculated from ¹H NMR spectroscopy data (Fig. 4A). To rationalize this result, we recorded the SEM-EDX spectrum of the product (Fig. 4D, Fig. S41 and Tables S5, S6, ESI†), which revealed presence of Rh metal and salt impurities that proved difficult to completely remove by our workup procedures. These impurities comprised of Rh, Na, Cl, and P in a 2:1:3:3 relative ratio, which partly explains the deviation of elemental

analysis data from expected. The observed Rh to Cl molar ratio is also supportive of minimal Cl content from the starting PVC. A duplicate reaction shows very similar results. To rule out any PVC remaining in the solution after the polymer product is precipitated, the material remaining in solution was characterized by ¹H NMR and ATR-IR spectroscopy. No unreacted PVC was identified. The mass of the polymer product (54 mg) was slightly higher to that expected for full conversion to PE (46 mg), which is explained from residual catalyst observed by EDX.

When using 1 equiv. of sodium hydride in lieu of sodium formate in THF at a 1 mol% catalyst loading, minimal activation of PVC was observed after 2 d at 110 °C (Fig. 3), which may be due to the poor solubility of NaH in THF. This prompted us to use N_iN -dimethylacetamide (DMA) as an alternative solvent that could better dissolve both PVC and NaH. ¹⁹ Nevertheless, reactions in DMA with 1 equiv. of NaH at 110 °C and 1 mol% catalyst loading for 2 d resulted primarily in DHC with minimal HDC discernible in the IR spectrum of isolated products (Fig. 3), which may be due to the much higher pKa of NaH. The weight of the polymer product (124 mg) and the residues left in solution (229 mg) are much larger than the mass of the starting reaction, which could be indicative of oxidation of the PA-like products.

Calculations identified that DHC with NaH alone (in THF and DMA) had the lowest barrier of conditions studied, while Rh-mediated DHC was calculated to have a much higher energy barrier and did not involve the use of NaH. To test these hypotheses, control reactions were performed using (xant-phos)RhCl and NaH individually with PVC in DMA, in addition

After Refore B. After

Materials Horizons

Fig. 5 Optimized NaHCO2 conditions resulted in full dechlorination of dyed PVC toy lizards and almost full dechlorination of soft, colorless PVC bags. Shaded regions a, c, and f highlight the characteristic PE peaks for the symmetric and asymmetric C-H stretching, CH₂ bending and CH₂ rocking vibrations, respectively. 21 Shaded regions b, d, and e highlight the C=O stretching, C-O stretching, and C=C bending modes as products of undesired side reactions, respectively. Shaded region g highlights the C-Cl stretching mode

3000

2500

2000 1500

Wavelength (cm⁻¹)

1000

Before

3500

4000

to controls with solvent alone. The latter revealed DMA can promote DHC of PVC on its own after 2 d at 110 °C, according to IR spectroscopy (Fig. S23, ESI†), which is likely due to the basicity of the solvent. Addition of (xantphos)RhCl doesn't appear to affect the chlorine content significantly when compared to that in the DMA control (Fig. S25, ESI†). Presence of NaH without the catalyst, however, results in considerable increase in dechlorination (Fig. S30, ESI†), in agreement with our calculations. Surprisingly, this reaction reaches virtually complete dechlorination within 2 h in the presence of 5 mol% (xantphos)RhCl (Fig. S21, ESI†), suggesting that cooperative DHC with catalyst and NaH seems to be occurring. The accessibility of catalyst-mediated DHC experimentally counters prior computational studies indicating high energy barriers for DHC. This warrants future work to understand how the hydride source and catalyst can cooperatively promote DHC at similar rates to HDC. Comparisons of reactions using sodium hydride, sodium formate and triethyl silane, under identical conditions (5 mol% catalyst and 1 equivalent H source) in DMA for 2 h yield a dechlorination efficiency order of NaH > NaHCO₂ > Et₃SiH (Fig. S21, S17 and S11, ESI,† respectively).

To further investigate impacts of solvent, identical reactions with sodium formate in THF vs. DMA reveal expected diminished selectivity for HDC in DMA (Fig. S14 and S16, ESI,† respectively). DFT calculations, using an implicit solvation model to capture dielectric screening effects of solvent, show that the differences in TOFs between THF and DMA are within one order of magnitude. Therefore, the observed experimental differences likely stem from higher basicity of DMA, which was not captured in simulations.

With optimal catalytic conditions in hand for the efficient and controlled HDC of PVC, studies were expanded to commercial PVC items to address catalyst stability in the presence of dyes, plasticizers and other additives. Toy lizards were chosen to test the catalyst's ability to withstand PVC dyes and added paints while a soft, colorless bag was chosen to test the catalysts robustness to plasticizers. As shown in Fig. 5, DHC of painted lizard toys and flexible plastic bags under the optimized conditions with sodium formate led to similar results to those with laboratory grade PVC. Interestingly, the plasticizers in the bag sample seem to promote some dehydrochlorination side reactions while the dyes and paints in the lizard sample do not.

Conclusions

In summary, (xantphos)RhCl was identified as an active catalyst for the complete dechlorination of PVC. Depending on the hydride source and solvent used, dechlorination could be optimized to be selective for HDC (using Et₃SiH or NaHCO₂ in THF) or DHC (NaH in DMA). These studies demonstrate how design of appropriate catalytic conditions can enable environmentally friendly dechlorination of PVC, while also prioritizing the organic product. Future studies are needed to decrease the cost of the catalyst used and improve purification methods for the organic product.

Author contributions

M. E. F. supervised this project and contributed to the manuscript; N. G. B. and M. K. A. contributed equally, performing all experimental reactions and writing the manuscript. S. B. performed turnover frequency calculations. S. M. S. supervised computational work and contributed to the manuscript.

Conflicts of interest

There are no conflicts to declare.

Acknowledgements

Funding for this project was provided by the Wrigley Institute for Environmental Studies through a Faculty Innovator Award and Wrigley Sustainability Prize, University of Southern California (USC) and USC Women in Science and Engineering start-up funds, and the National Science Foundation (CHE-2203756). The X-ray crystallography data, described in the ESI,† was supported by the National Science Foundation (CHE-2018740). Computational work was supported by the Department of Energy (DE-SC0021417). SEM-EDX data was obtained by Amir Avishai at the USC Core Center for Excellence of Nano Imaging. We would also like to thank Rika Mizoguchi for her help with the Table of Contents graphic as a Wrigley Institute Environmental Communications intern.

Communication **Materials Horizons**

References

- 1 A. J. Martín, C. Mondelli, S. D. Jaydev and J. Pérez-Ramírez, Chem, 2021, 7, 1487-1533.
- 2 J. Hopewell, R. Dvorak and E. Kosior, Philos. Trans. R. Soc. London, Ser. B, 2009, 364, 2115-2126.
- 3 J. Yu, L. Sun, C. Ma, Y. Qiao and H. Yao, Waste Manage., 2016, 48, 300-314.
- 4 W. H. Starnes, Prog. Polym. Sci., 2002, 27, 2133-2170.
- 5 A. López, I. de Marco, B. M. Caballero, M. F. Laresgoiti and A. Adrados, Fuel Process. Technol., 2011, 92, 253-260.
- 6 A. Lopez-Urionabarrenechea, I. de Marco, B. M. Caballero, M. F. Laresgoiti and A. Adrados, J. Anal. Appl. Pyrolysis, 2012, 96, 54-62.
- 7 D. Ma, L. Liang, E. Hu, H. Chen, D. Wang, C. He and Q. Feng, Process Saf. Environ. Prot., 2021, 146, 108-117.
- 8 L. Guo, G. Shi and Y. Liang, *Polymer*, 2001, 42, 5581–5587.
- 9 D. L. Allara and W. L. Hawkins, ed., Stabilization and Degradation of Polymers, American Chemical Society, Washington, DC, 1978, vol. 169.
- 10 W. H. Starnes, F. C. Schilling, K. B. Abbås, I. M. Plitz, R. L. Hartless and F. A. Bovey, Macromolecules, 1979, 12, 13-19.
- 11 R. E. Cais and C. P. Spencer, Eur. Polym. J., 1982, 18, 189-198.
- 12 T. Hjertberg and A. Wendel, Polymer, 1982, 23, 1641-1645.
- 13 F. A. Jameison, F. C. Schilling and A. E. Tonelli, Macromolecules, 1986, 19, 2168-2173.
- 14 J. D. Cotman, J. Am. Chem. Soc., 1955, 77, 2790-2793.
- 15 J. M. Contreras, G. Martínez and J. Millán, *Polymer*, 2001, 42, 09867-09876.
- 16 L. Monsigny, J.-C. Berthet and T. Cantat, ACS Sustainable Chem. Eng., 2018, 6, 10481-10488.
- 17 S. G. Curto, L. A. de las Heras, M. A. Esteruelas, M. Oliván and E. Oñate, Organometallics, 2019, 38, 3074-3083.
- 18 S. Bac, M. E. Fieser and S. Mallikarjun Sharada, *Phys. Chem.* Chem. Phys., 2022, 24, 3518-3522.

- 19 G. Grause, S. Hirahashi, H. Toyoda, T. Kameda and T. Yoshioka, J. Mater. Cycles Waste Manage., 2017, 19, 612-622.
- 20 M. P. Wilkerson, C. J. Burns, R. T. Paine and B. L. Scott, Inorg. Chem., 1999, 38, 4156-4158.
- 21 A. Misono, Y. Uchida and K. Yamada, BCSJ, 1970, 43, 3259-3262.
- 22 A. Misono, Y. Uchida and K. Yamada, BCSJ, 1967, 40, 2696-2698.
- 23 A. Misono, Y. Uchida and K. Yamada, BCSI, 1966, 39, 2458-2463.
- 24 D. Braun, W. Mao, B. Böhringer and R. W. Garbella, Angew. Makromol. Chem., 1986, 141, 113-129.
- 25 N. Pourahmady, P. I. Bak and R. A. Kinsey, J. Macromol. Sci., Part A: Pure Appl. Chem., 1992, 29, 959-974.
- 26 P. V. C. Rao and V. K. Kaushik, Polym. Test., 1999, 18, 429-438.
- 27 A. Misono, Y. Uchida and K. Yamada, BCSI, 1970, 43, 3597-3601.
- 28 M.-F. Llauro-Darricades, N. Bensemra, A. Guyot and R. Petiaud, Makromol. Chem., Macromol. Symp., 1989, 29,
- 29 F. C. Schilling, A. E. Tonelli and M. Valenciano, Macromolecules, 1985, 18, 356-360.
- 30 D. Li, L. Zhou, X. Wang, L. He and X. Yang, Materials, 2019, 12, 1746.
- 31 S. Siddique, G. D. Smith, K. Yates, A. K. Mishra, K. Matthews, L. J. Csetenyi and J. Njuguna, J. Polym. Res., 2019, 26, 154.
- 32 M. A. Yusof, N. H. N. Rahman, S. Z. Sulaiman, A. H. Sofian, M. S. Z. M. Desa and I. Izirwan, 2018 IEEE 9th International Conference on Mechanical and Intelligent Manufacturing Technologies (ICMIMT), IEEE, Cape town, South Africa, 2018, pp. 6-9.